An investigation of the elastoplastic nature of ITD on the toughness of the dentin microstructure

BY

Hanfeng Zhai

Department of Mechanics,
School of Mechanics and Engineering Science,
Shanghai University

RESEARCH

Submitted as a scientific report

for the *SHU summer research program*, 2020

Dr. Bingbing An

CONTENT

An investigation of the elastoplastic nature of ITD on the toughness of the dentin microstructure

Abstract

Dentin is an essential part of the human tooth that displays superior mechanical behaviors such as high stiffness and toughness relative to its lightweight, attributed to its microscopic structure. Here, we adopt the elastic and perfectly plastic model for ITD and ductile damage evolution model for material failure. We calculate the stiffness of the dentin through consider it as composite materials. The tensile loading simulation indicates that dentin structure with plastic ITD will generate strain concentration along with the four corners on ITD bonging PTD. The plasticity will reduce the forces acting on the structure. There are crack occurs on PTD initiated along the DT edge to the axis perpendicular to the loading direction, which corresponds to the stress concentration as on the unit cell model. There are wavy cracks on the ITD nearing the bonding interface between ITD and PTD. Most generated cracks evolved from the DT edge propagating on PTD till further on ITD. The ITD plasticity makes the stress-strain more evenly distributed on the structure in crack propagation. The quantitative results indicate the ITD plasticity can reduce the stress on PTD as to resist crack growth but make little effect on the stress of ITD as the growing strain. The ITD plasticity makes a little variation on the shear stress distribution on the bonding interface, indicating such nature does not contribute to the debonding effect as a major role.

Keywords*:* biomechanics; biomaterials; composite materials; dentin; microstructure

1 Introduction

Biomaterials display superior mechanical behaviors adjusting to its loading conditions with millions of years of evolution. Tooth, as one of the most common characters seen from most creatures, exhibits high fracture resistance, containing enamel and dentin [1]. The enamel and dentin exhibit extremely different structures containing different chemicals adjusting to their different functions. The dentin evolving to convey nutrition as to supply the enamel and the whole tooth structure [2]. Also, it will absorb energy from enamel from chewing as the cracks propagating in enamels. The dentin microstructures consist of void rounded by hard materials embedded in soft materials [2]. Most biomaterials display plasticity as to resist failure. The biomaterials can be depicted by multiple models including the Drucker-Prager yield function ([3], [4], [13], [14], [15], [16], [17]). The fracture and crack growth can also be depicted by many models ([5], [6], [7]). In fine, many developed mechanical models can be adopted for delineating the biomaterials behavior.

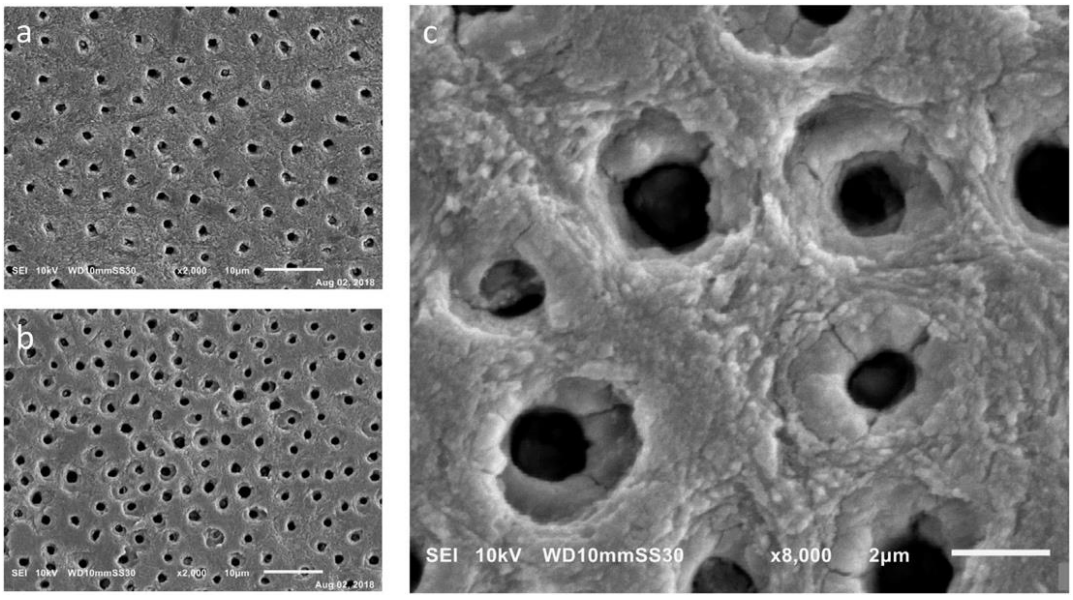

Fig. 1 SEM photos of the dentin microstructure, taken by A. Nazari *et al.* [12]

Specifically, dentin structure mechanical behavior is well studied through experimental approaches ([9], [10]). The measured Young's Modulus, Yield stress, etc. from published resources is adopted in our study. The zoomed view of SEM photos shows good details of the dentin microstructure ([11], [12]). From the SEM photos as given in Fig. 1, we observe basic characteristics of the dentin microstructure: consisting of small voids surrounded by larger circular edges, further embed in matrix materials. The fracture behavior is comprehensively studied by An with the adoption of the Drucker-Prager criterion ([13], [15], [16], [17]). Notably, two types of fracture: cracks occur on PTD initiated on the DT edge, which is also detected through SEM photos ([11], [12]); and the cracks propagated along with the ITD and PTD bonding interface caused by the elastic moduli mismatch [13]; are specifically detected through the work by An through numerical approaches.

As studied, the dentin and other biomaterials can be seen as composites consisting of materials with different properties. With the previous introductions, the plasticity of the dentin can be elicited as to study the fracture behavior. The elastoplastic behavior of composite indicates their mechanical behaviors ([18], [19], [20]). In our approaches, we follow the basic modeling strategy as previous studies conducted by An ([13], [15], [16], [17]). The main focuses are on the investigation of the ITD elastoplastic nature as its functions in affecting the composite's stiffness and toughness. To simplify, we adopt perfectly plasticity for ITD and ductile damage model for evolution. The approaches may not perfectly satisfy the experimental results, howbeit still offer decent insights for investigations of the ITD plasticity on dentin microstructure.

2 Method

2.1 Stiffness and strength

2.1.1 Elastic ITD

As discussed in §1, preceding studies show that the dentin structure involves a special hierarchical structure include a void nominated as Dentin Tubule (DT) surrounded by a round of hard materials called Inter-Tubular Dentin (ITD), and embedded in soft materials called Peri-Tubular Dentin (PTD). The microscopic scale dentin is generally consisting of thousands of such similar structures, which we considered as a "unit cell" for the structure. To investigate the mechanics of the dentin, we model such a unit cell as shown in Fig. 2 for simulations and calculations.

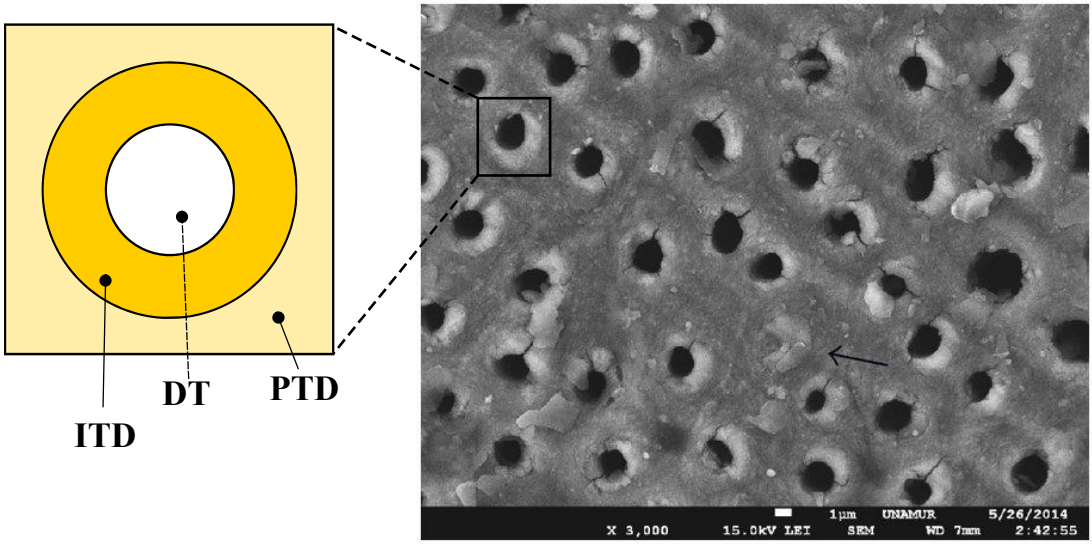

Fig. 2 Schematic view for the basic modelling strategy of the dentin unit cell, nominating each part as shown. The SEM photo is taken by A. Namour *et al.* [11]

Initially, the dentin microstructure can be seen as composite materials with bonded materials of different modulus. To calculate the stiffness of such a composite structure, we carry out loadings on the unit cell structure as shown in Fig. 3. Note that the boundary conditions can be written as:

$$\begin{cases} y = 0\colon\ u_2 = 0 \\ x = \pm m\colon\ u_1 = 0 \\ y = n\colon u_2 = +1 \end{cases} \tag{1}$$

With the boundary conditions, we load the unit cell with a 2-directional unit displacement. With the loading, we can calculate the mean stress and mean strain in the 2-direction as:

$$\bar{\varepsilon}_y = \frac{u_y}{m} \tag{2}$$

$$\bar{\sigma}_y = \sum_{x=0}^{a} \frac{R_y(x,n)}{m} \tag{3}$$

Henceforth, the elastic modulus of the composite materials as:

$$E_y = \frac{\bar{\sigma}_y}{\bar{\varepsilon}_y} \tag{4}$$

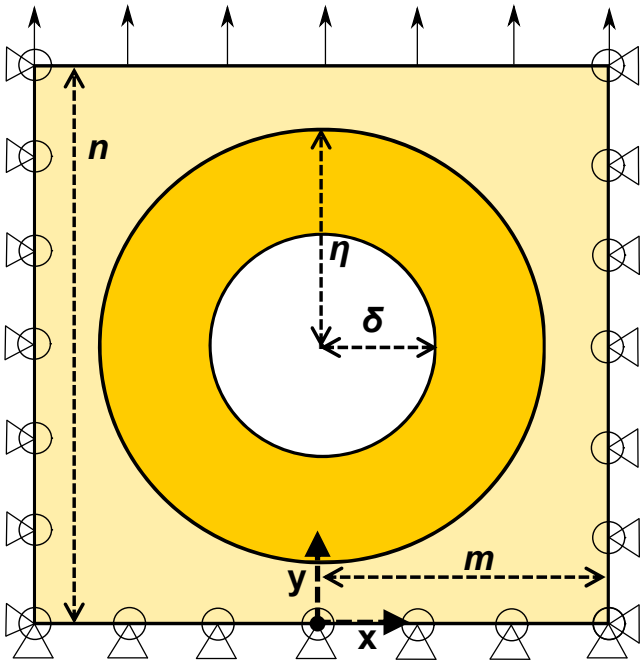

Fig. 3 Schematic illustration of the unit cell undergoing mechanical loadings for calculation of the composite's Young's modulus. Note that the geometric parameters: $\delta = 2, \eta = 4, m = 5, n = 2m$, in μm. Note that x axis is also recognized "1-direction", y axis is also recognized "2-direction".

As introduced in §1, we know that the ITP and PTD have different Young's modulus, indicate different stiffness. Here, we present parameters for the dentin's ITP and PTD as shown in Tab. 1 and Tab. 2 based on previous studies ([14], [15]). Note that

the modulus value is chosen within an experimental data range and the yield stress is neglected in 2.1.1 as considering an elastic ITD.

Youngs modulus	Poisson's ratio
200GPa	0.3

Tab. 1 The mechanical parameter for PTD.

As given in Tab. 1, the PTD is considered as a pure elastic material.

Youngs modulus	Poisson's ratio	Yield stress
20GPa	0.3	70MPa

Tab. 2 The mechanical parameter for ITD, where the yield stress denote the plastic attribute of ITD, which is considered separately.

2.1.2 Plastic ITD

From §1 we know that the plastic nature of the dentin ITD is adopted or ignored with regards to the specific topics studied by previous scholars. In this part, to delineate such an effect on the composite's stiffness, we adopt the plastic nature of the ITD compared to 2.1.1. Note that a perfectly plastic model is adopted to simplify the estimation and neglect the complex hardening or softening effect.

Here, for the strain of the plastic model can be depicted as:

$$\boldsymbol{\varepsilon} = \boldsymbol{\varepsilon}^e + \boldsymbol{\varepsilon}^p \tag{5}$$

Therefore, the stress can be written as

$$\boldsymbol{\sigma} = \boldsymbol{C}: (\boldsymbol{\varepsilon} - \boldsymbol{\varepsilon}^p) \tag{6}$$

As mentioned, a perfect plasticity model is adopted. When the stress is in within the yield strength, such condition is represented as the plastic strain does not change:

$$d\boldsymbol{\varepsilon}^p = 0 \tag{7}$$

When the stress reaches the yield strength in tension, in uniaxial problem, the plastic strain can only increase and the 2-directional stress equals the yield:

$$d\boldsymbol{\varepsilon}^p > 0, \qquad \frac{\sigma_{22}}{\sigma_Y} = 1 \tag{8}$$

Where σ_Y denotes the yield stress, and σ_{22} is the 2-directional stress.

We adopt such a model just to study how the plasticity might influence the dentin's stiffness in this section. Here, we apply the yield stress as given in Tab. 2 for the ITD and carrying out simulations for the same model as shown in Fig. 3. To specify, the PTD is considered as a purely elastic material due to its higher stiffness, the yield stress effect is not required in the study of composite's stiffness. Note that both the simulations in 2.1 are carried out in Abaqus/CAE 2017. For the meshing, we adopt the Plane strain assumption, with mesh-type CPE4.

2.2 Toughness and fracture

2.2.1 Elastic ITD

Numerous studies ([2], [13], [15], [16], [17]) indicate that dentin structure displays high fracture resistance and such specific mechanical property is widely studied both experimentally and numerically. Here, a simplified failure model for crack propagation is adopted as an energy-based, linear softening, hybrid mode damage evolution model, where the criterion for damage initiation is when the maximum principal stress reaches a specific value.

For the damage evolution, we adopt a ductile damage model, in which the equivalent plastic strain is a function of strain rate and stress triaxiality:

$$\dot{\boldsymbol{\varepsilon}}_D^p = \dot{\boldsymbol{\varepsilon}}_D^{pl}(\eta,\ \dot{\boldsymbol{\varepsilon}}^p) \tag{9}$$

Where the stress triaxiality is a division of hydrostatic stress to von Mises stress:

$$\eta = \frac{J_1}{\sigma_v} \tag{10}$$

And the damage evolves when:

$$w_D = \frac{d\dot{\boldsymbol{\varepsilon}}^p}{\dot{\boldsymbol{\varepsilon}}_D^{pl}(\eta,\ \dot{\boldsymbol{\varepsilon}}^p)} = 1 \tag{11}$$

In which w_D is an increment variable increasing with plastic strain:

$$\Delta w_D = \frac{\Delta\dot{\boldsymbol{\varepsilon}}^p}{\dot{\boldsymbol{\varepsilon}}_D^{pl}(\eta,\ \dot{\boldsymbol{\varepsilon}}^p)} \geq 0 \tag{12}$$

For the damage initiation model, the maximum principal stresses for PTD and ITD are shown in Tab. 3 and Tab. 4, respectively.

Youngs modulus	Poisson's ratio	Maximum principal stress
200GPa	0.3	86MPa

Tab. 3 The parameters of PTD for fracture simulation.

Youngs modulus	Poisson's ratio	Maximum principal stress
20GPa	0.3	10MPa

Tab. 4 The parameters of ITD for fracture simulation.

For our model, the equation for the energy of crack propagation:

$$KE = \int_{a_0}^{a} (G - R)\, da \tag{13}$$

In which G is the energy dissipative rate, R is the fracture energy denoted as $R = G_{ic}$. In our model, we adopt that $G_{1c} = G_{2c} = G_{3c}$ as given in Tab. 5 and Tab. 6.

The crack propagation rate is given as:

$$\dot{a} = \sqrt{\frac{2\pi}{\alpha}} \cdot \sqrt{\frac{E}{\rho}} \cdot \left(1 - \frac{a_0}{a}\right) \tag{14}$$

As mentioned, in our model, we adopt a linear damage model, hence we have $\alpha = 1$ as shown in Tab. 5 and Tab. 6.

Normal mode	Shear mode		
Fracture energy	Fracture energy (1-direction)	Fracture energy (2-direction)	Power
43000	43000	43000	1(Linear)

Tab. 5 The parameters of PTD for fracture simulation.

Normal mode	Shear mode		
Fracture energy	Fracture energy (1-direction)	Fracture energy (2-direction)	Power
5000	5000	5000	1(Linear)

Tab. 6 The parameters of ITD for fracture simulation.

For 2.2.1, we adopt the same strategy as in 2.1.1, that the plastic nature of ITD is neglected. Hence, a fracture occurs on ITD and is considered as elastic failure. The mechanical model carried out for fracture of the dentin microstructure is shown in Fig. 4. Note that the model consists of 54 "unit cells" as shown in Fig. 3.

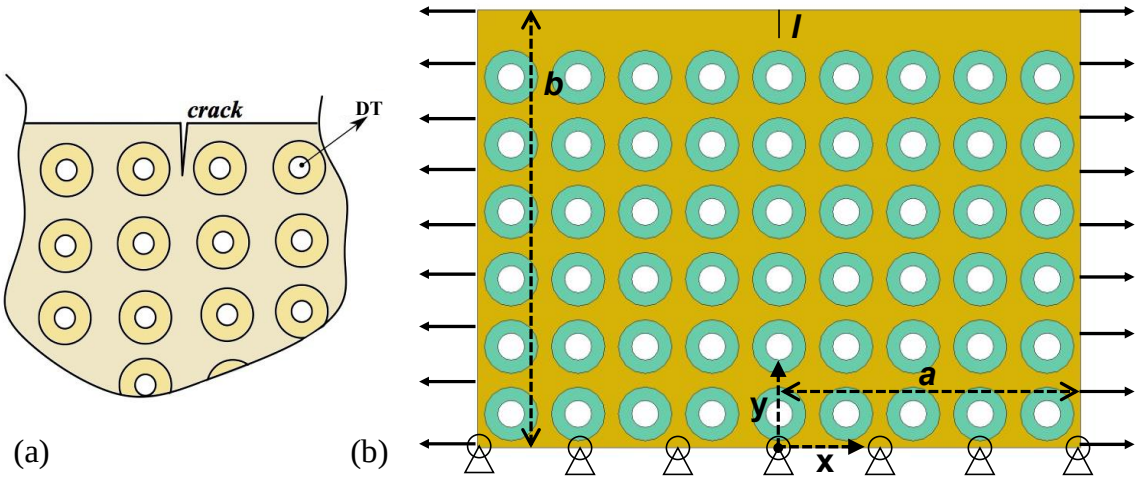

Fig. 4 Schematic view of the mechanical model carried out for fracture simulation. (a) Schematic for the crack initiation on dentin. (b) Mechanical model for the fracture simulation, in which the 1-directional loading is $u_{-1} = -1,\ u_{+1} = 1$. Note that the initial crack length $l = 5$, in μm. Note that x axis is also recognized "1-direction", y axis is also recognized "2-direction".

The boundary conditions for our mechanical model can be mathematically written as:

$$\begin{cases} y = 0\text{: } u_2 = 0 \\ x = \pm a\text{: } u_1 = \pm 1 \\ y = b\text{: } F_s = 0 \end{cases} \tag{15}$$

In which F_s denotes the surface force acting on the edge.

2.2.2 Plastic ITD

In this part, we adopt similar strategies as given in 2.1.1 to 2.1.2. We neglect the ITD's plastic nature in 2.2.1. Here, we set the ITD as perfectly plastic material as given in Tab. 2. With the set plastic ITD and elastic PTD, we carry out the same simulation with the same mechanical loadings as given in Fig. 4 and Eq. 15, with the same initial crack, with length $l = 5$.

Note that both the simulations in 2.2 are carried out in Abaqus/CAE 2017. For the meshing, we adopt the Plane strain assumption, with mesh-type CPE4.

3 Results and discussion

3.1 Stiffness and strength

3.1.1 Elastic ITD

With the mechanical loadings as given in Fig. 3 and Eq. 1, we obtain results as shown below. From Fig. 5 and Fig. 6 we got the strain and stress distribution on the dentin unit cell from the first and last step as given from (a) to (b).

From the strain distribution as given in Fig. 5 one can observe that applied with an elastic ITD, the 2-directional strain is concentrated along the central axis in 2-direction, while displays a generally low value along the on the ITD. Albeit the strain is concentrated along the 1-direction's edge on the PTD along with the DT.

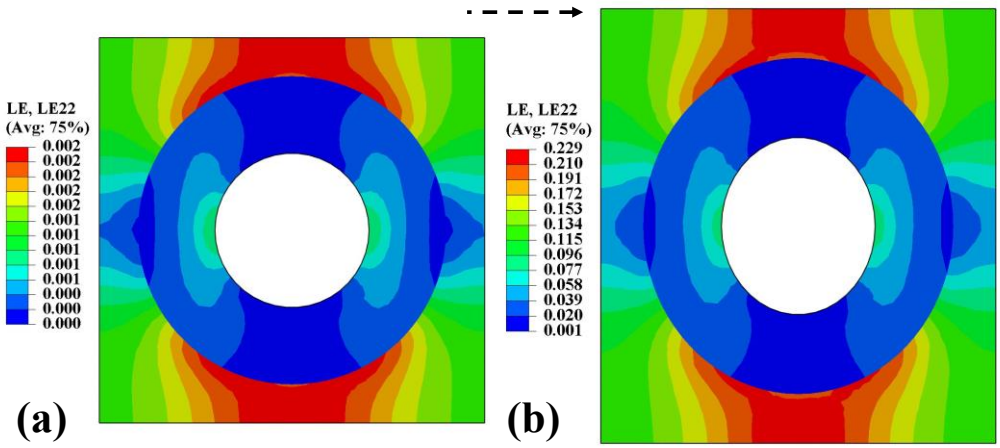

Fig. 5 The 2-directional strain distribution of the unit cell under uniaxial loading, with elastic ITD. (a) First step. (b) Last step.

From the 2-directional stress distribution as given in Fig. 6, one discerns that the stress is concentrated along the 1-direction along the DT edge on PTD. Such a phenomenon indicates higher possibilities for the fracture to occur on PTD along the axis perpendicular to loading directions under tensile loadings. The 1-directional stress value on ITD is low compared with the total stress distribution. We also find that the 2-directional stress is more evenly distributed with the loadings from (a) to (b).

The elastic ITD exhibits similar stress-strain distribution from the beginning to the end of the loading as shown from (a) to (b) in Fig. 5 and Fig. 6.

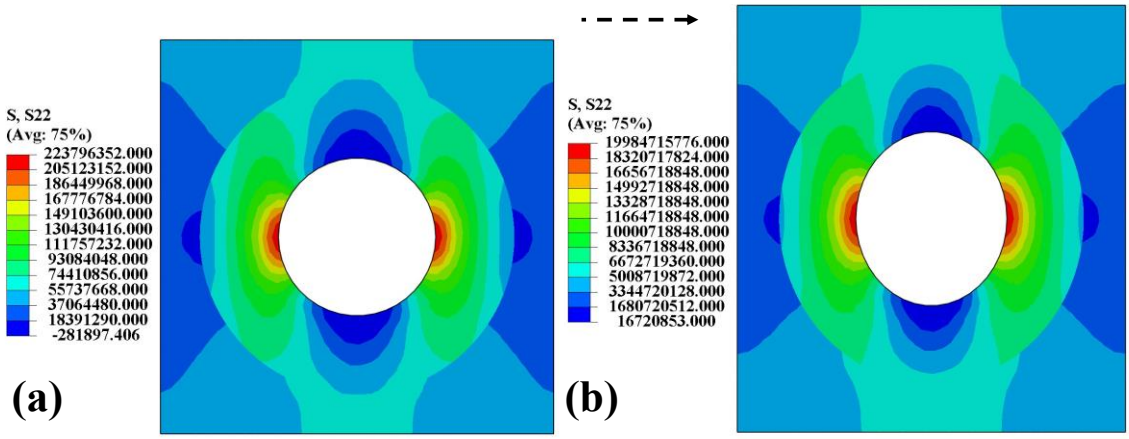

Fig. 6 The 2-directional stress distribution of the unit cell under uniaxial loading, with elastic ITD. (a) First step. (b) Last step.

3.1.2 Plastic ITD

Here, as given from Eq. 5 to Eq. 8 and in Tab. 2, we adopt a perfectly plasticity model for ITD for the same uniaxial loading to check how plasticity influences the 2-directional stress-strain distribution as compared with Fig. 5 and Fig. 6. As shown in Fig. 7, we discern that the 2-directional strain has the same distribution in the first step with the elastic ITD as compared with Fig. 5(a). However, as the loading keeps, the plastic ITD displays a totally different strain distribution, shown in Fig. 5(b). We observe that the strain is robustly concentrated along the PTD edge on the four corners. Also, the total strain value is increased with the plastic effect. For what is more, the total strain is distributed concentrating on the four edges tangent to the PTD circular edge. Such a phenomenon indicates a protection mechanism for the ITD to constrain the failure.

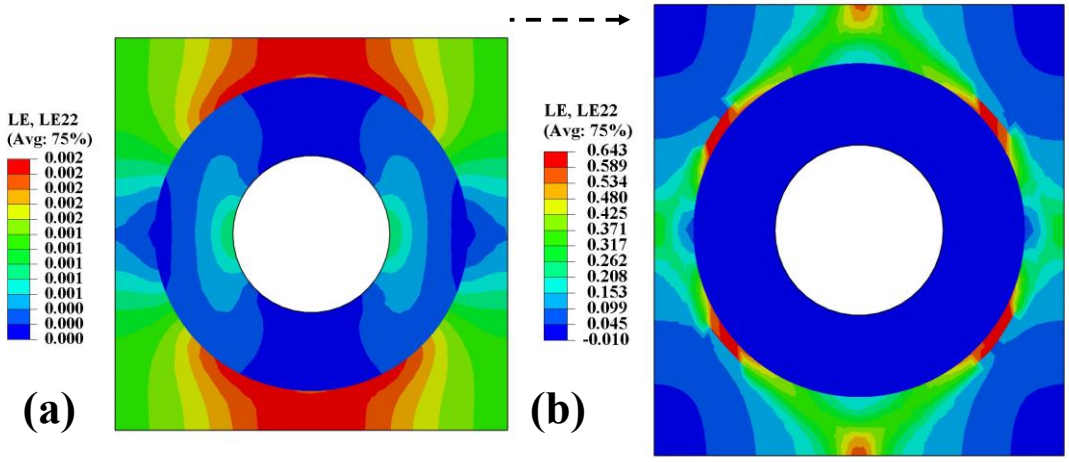

Fig. 7 The 2-directional strain distribution of the unit cell under uniaxial loading, with perfectly plastic ITD. (a) First step. (b) Last step.

As mentioned, comparing Fig. 7(b) with Fig. 5(b) one discern extremely different strain distributions. To delineate such, we calculate the plastic strain of the unit cell as shown in Fig. 8 From Fig. 8(b) and Fig. 7(b) we deduce that plastic strain plays a

major role in the total 2-directional strain based on the fact that the two figures exhibit similar patterns. Moreover, from Fig. 8 we observe that the plastic strain initiated along the lines that tangent to the PTD circular edge and evolving from closer to the 2-direction's concentration to a more evenly distributed pattern. Such plastic strain could help explain how the plastic nature could help restrain the fracture.

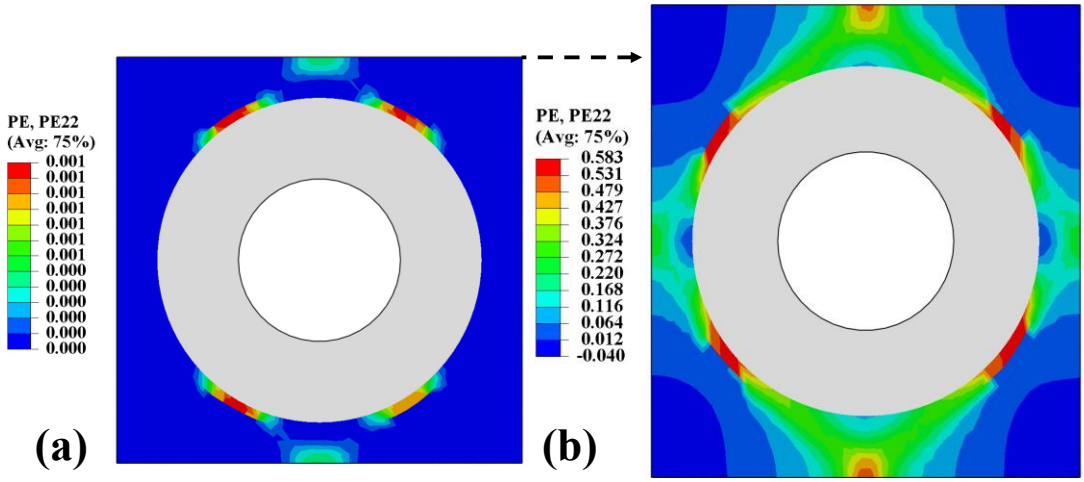

Fig. 8 The 2-directional plastic strain distribution of the unit cell under uniaxial loading, with perfectly plastic ITD. (a) First step. (b) Last step.

Similarly, we also present how the 2-directional stress evolves on the unit cell with a plastic ITD. As comparing Fig. 9(a) with Fig. 6(a) we also discern the same stress distribution at the beginning stage. However, as given in Fig. 9(b) and Fig. 6(b), we observe that the total 2-directional stress value is greatly reduced due to the plastic nature of ITD. The stress is also more evenly distributed among the unit cell. Notably, the 2-directional stress is also highly concentrated along the 1-direction on the PTD, but such stress value is highly reduced compared with Fig. 6(b). Though the PTD material properties remain the same, the ITD properties' change contends an alleviation of the stress concentration on the PTD.

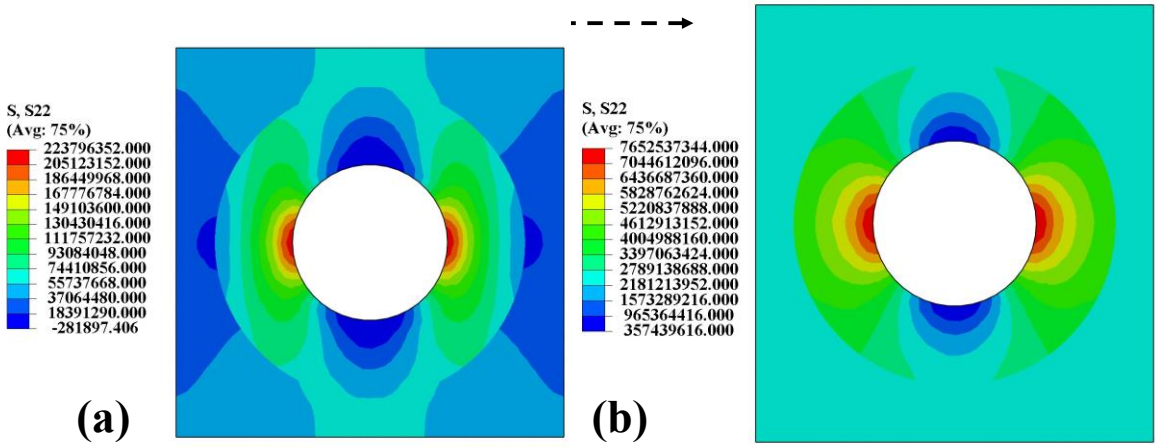

Fig. 9 The 2-directional stress distribution of the unit cell under uniaxial loading, with perfectly plastic ITD. (a) First step. (b) Last step.

Based on Eq. 2 to Eq. 4 we obtain results from Fig. 10, indicating how stiffness evolve with the loading.

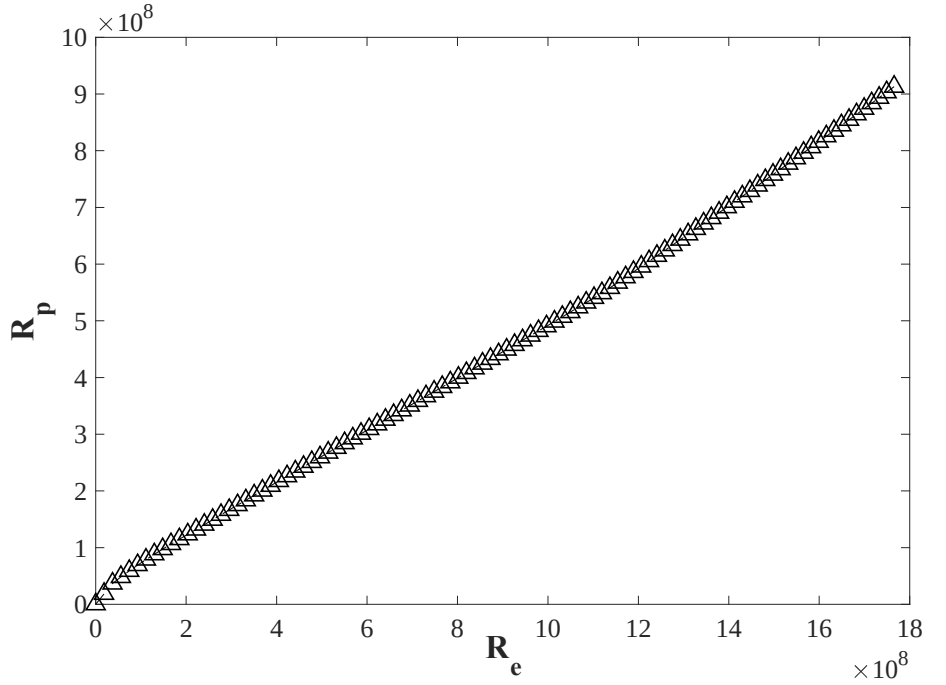

Fig. 10 The relationship between the reaction force with the model of elastic ITD and perfectly plastic ITD, in which R_e represents reaction force for elastic ITD and R_p represents reaction force for plastic ITD. Note that the unit is 10^{12} N.

From Fig. 10, the slope $\frac{\mathrm{d}R_p}{\mathrm{d}R_e}$ initially grows and the steepness decreases in the when R_e reaches the value around 3, the slope started to decrease, indicating the ITD's plastic nature started to make effect on the loading. When R_e reaches the

value around 12, it started to increase again yet the value is still below 1 indicate that $R_p < R_e$, we can explain such a phenomenon as the ITD's plastic effect does not exhibit as evident as the beginning stage yet still make an effect on the composite's total stiffness.

3.2 Toughness and fracture

3.2.1 Elastic ITD

Based on the damage evolution model (Tab. 3 – Tab. 6) and mechanical loadings (Fig. 4), we obtain results as given indicating how fracture initiate and develops on the dentin structure as shown below. Fig. 11 – Fig. 13 shows the fracture evolution of the 1-directional stress distribution on the dentin structure.

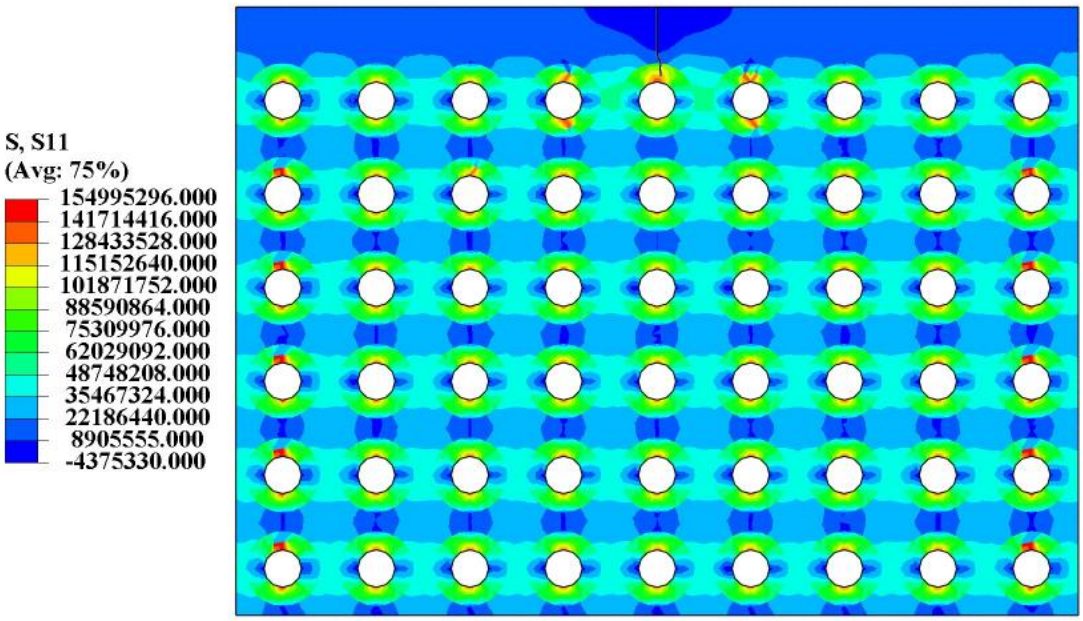

Fig. 11 The 1-directional stress distribution of preliminary stage of the crack propagation on dentin structure, with elastic ITD.

Fig. 11 shows that the 1-directional stress generally has the same distribution around the DT referring to such distribution on unit cell (Fig. 6). Notwithstanding, there is some detectable stress concentration on the PTD along the 2-direction near

the initial crack. Such a phenomenon could be explained by the initial crack propagation effect, in which the crack surrounding area absorbs more energy from fracture.

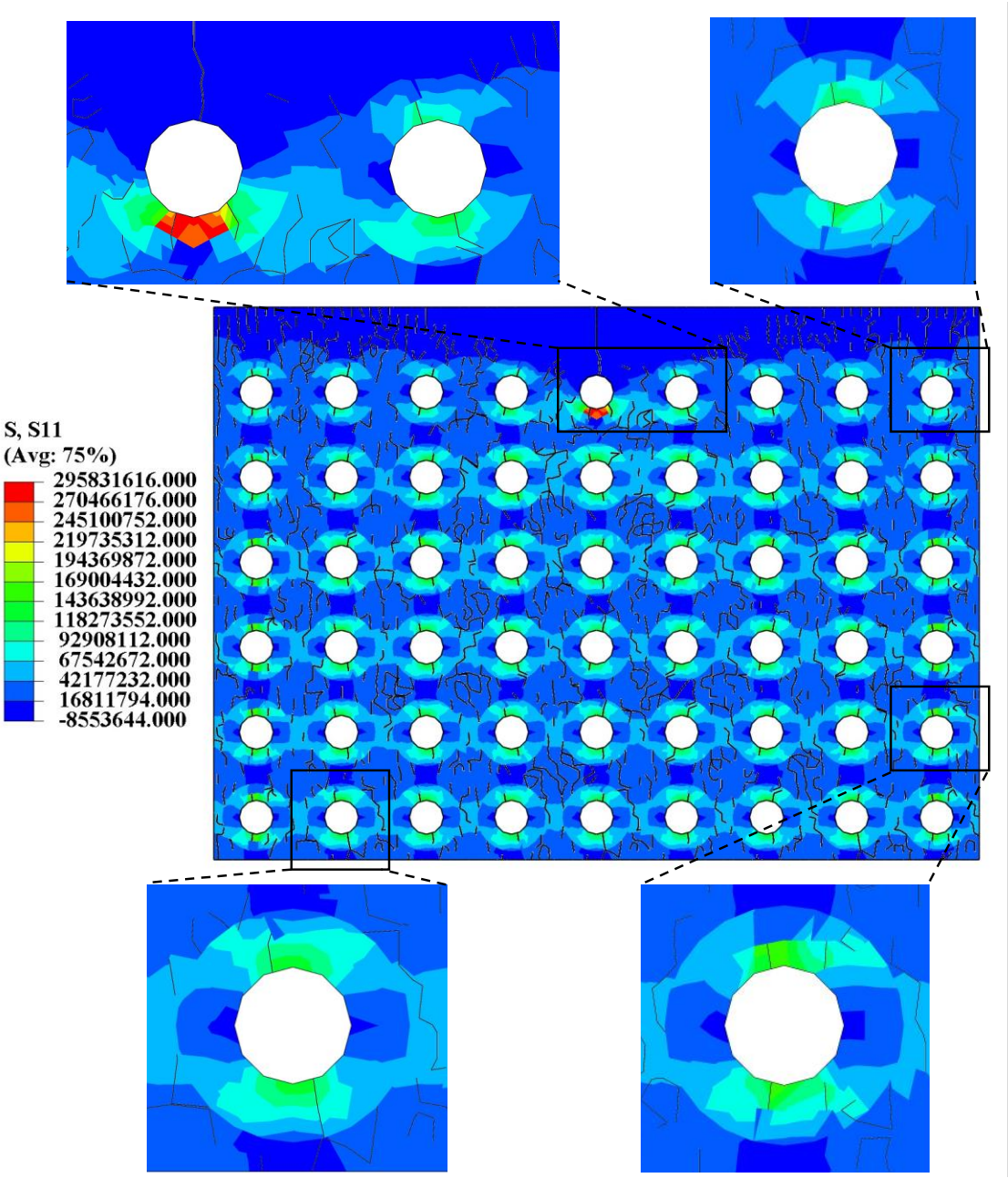

Fig. 12 The 1-directional stress distribution, when the fracture initiate on dentin, in which the zoomed view shows the how cracks evolved around the DT, with elastic ITD.

From Fig. 12 one observes how cracks initiated on the dentin microstructure. From the zoomed view on the right top part, we detect the DT bonding the initial crack has a stress concentration on the PTD in the lower part. Also, from the

neighboring DT one observes cracks propagated along the axis perpendicular to the loading directions, which have been discussed in 3.1. Such a similar pattern is also detected on the other zoomed views in Fig. 12 which is studied by other scholars ([2], [12], [13]) For what is more, the 1-directional stress value is lower on PTD under same direction's loading, observed from the two down zoomed views. Such distribution is also explained in 3.1 as tensile loading on the unit cell. Aside from the perpendicular directional cracks, there are cracks on ITD close to the PTD with a wavy shape in the right-top and down zoomed views. Such cracks could indicate a debonding between the ITD and PTD, but not the exactly debonding effect explained as elastic modulus mismatch ([15], [16]), could be attributed to the mechanical model.

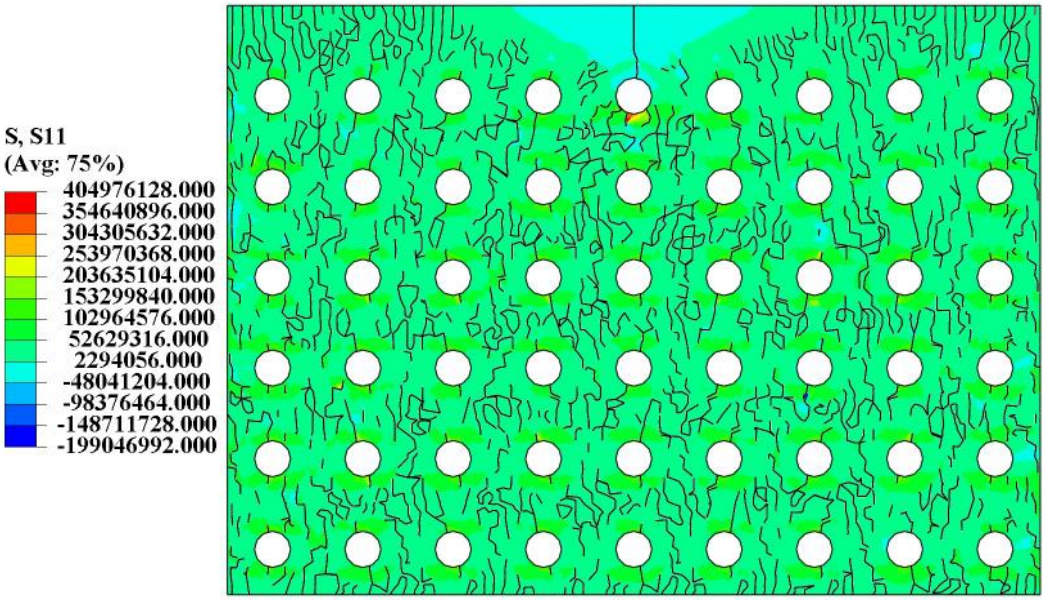

Fig. 13 The 1-directional stress distribution of the final stage of the fracture on dentin's microstructure, with elastic ITD.

In Fig. 13, the crack is fully propagated on the dentin, in which we observe more evenly distributed 1-directional stress and mildly higher stress value on the PTD along the 2-direction. Also, some cracks perpendicular to the loading directions on the

PTD propagated on the ITD and connected with the mentioned wavy cracks that may be related to the debonding. Such indicates how cracks on ITD is propagated from cracks originated from DT on the PTD. Notably, the DT neighboring the initial crack generates more crack in the lower part compared with the step of fracture initiation.

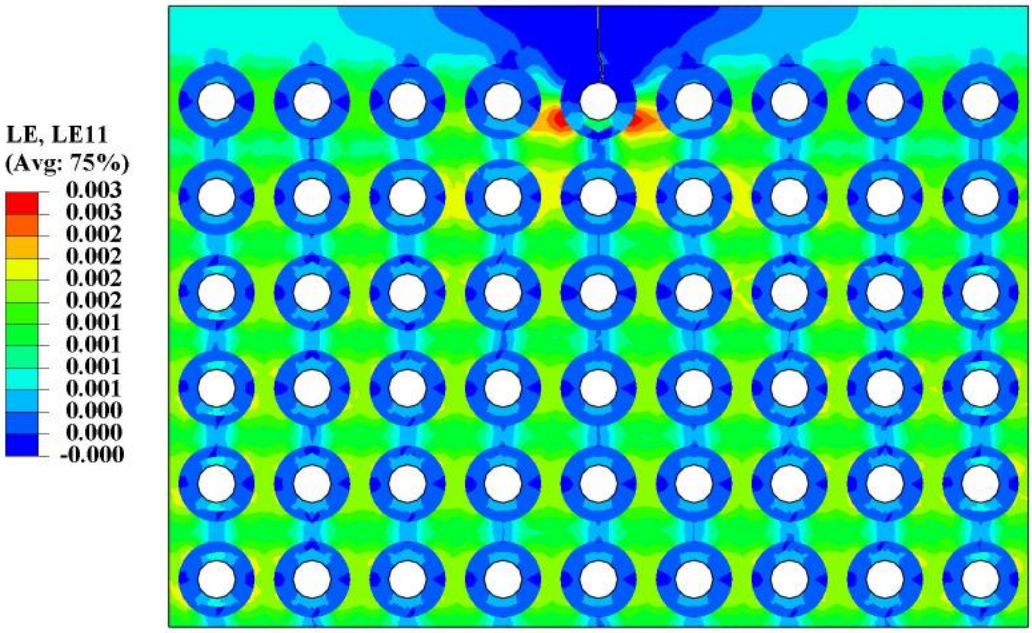

Fig. 14 The 1-directional strain distribution of preliminary stage of the crack propagation on dentin structure, with elastic ITD.

In Fig. 14, we observe a larger value of 1-directional strain on the ITD comparing with PTD due to the smaller elastic modulus. There are also strain concentrations along with the DT neighboring the initial crack. Notably, a severe 1-directional strain concentration on the ITD bonding the DT neighboring the initial crack can be detected. Also, we observe a larger strain value in 2-direction on PTD surrounding the DT. Correspondingly, a smaller strain value in 2-direction on ITD. In detail, there are 1-directional strain concentration occurs around the DT neighboring the initial crack for a value of about 0.002. Such patterns are also discerned in the lower part occurs on ITD bonding the PTD, such strain indicates the possibility of the debonding.

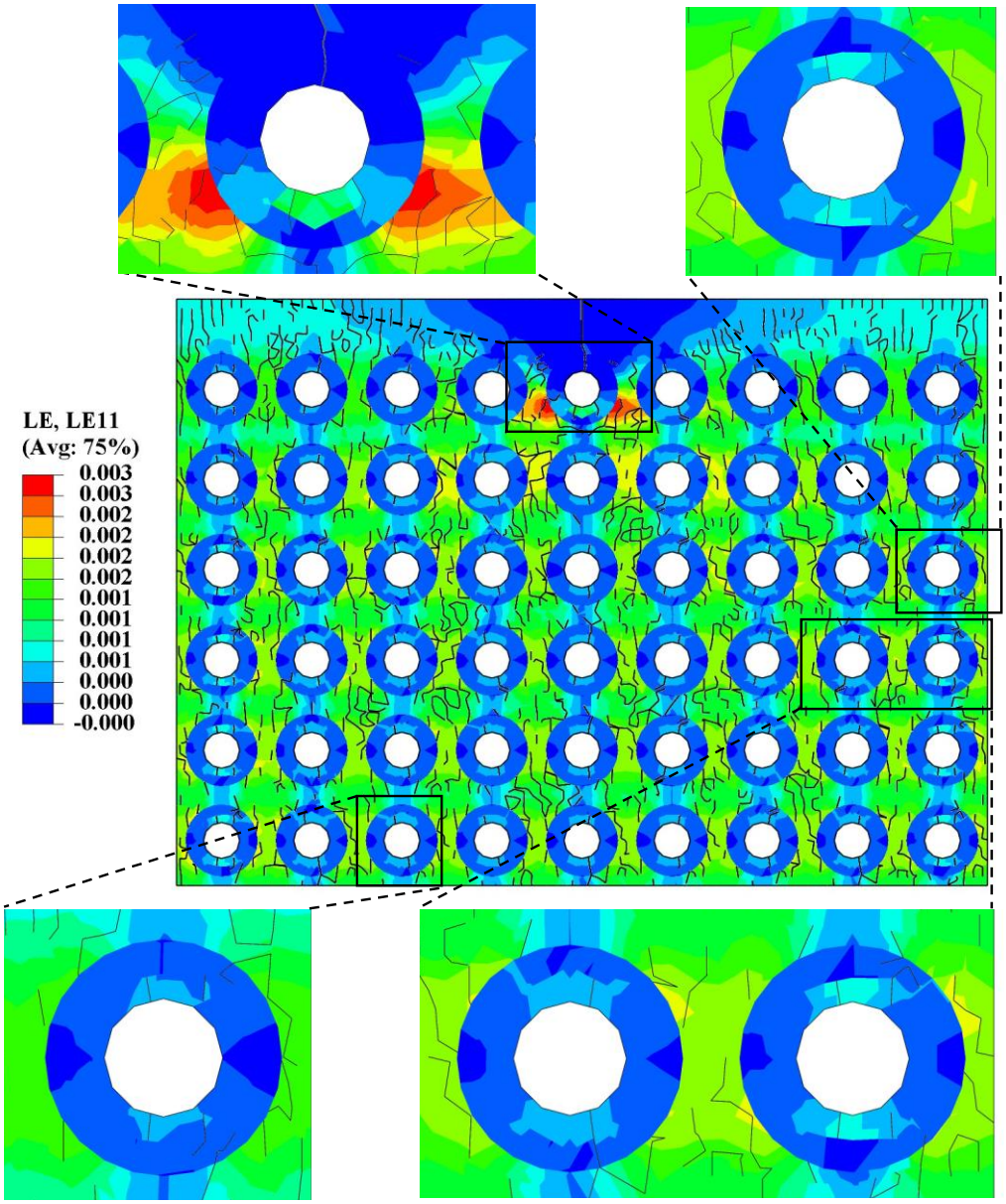

Fig. 15 The 1-directional strain distribution, when the fracture initiate on dentin, in which the zoomed view shows the how crack evolved around the DT, with elastic ITD.

From the 1-directional strain distribution as the same step as in Fig. 12 shown in Fig. 15, we observe evident strain concentration on the ITD bonding the DT neighboring the initial crack. Such a phenomenon, corresponding to Fig. 12, as the stress concentration occurs on the PTD of the same DT, could reflect the stiffness difference of ITD and PTD. Notably, we observe cracks parallel to loading direction as shown in

the right-top and right-down zoomed views. The cracks can be attributed to the inner friction of the PTD under 1-directional loading. As shown in the left-top zoomed view, there is a "V-shaped" crack occurs on the PTD neighboring the initial crack, the "V-shape" could be explained as the synergy of the PTD inner friction and the propagation and the fracture energy dissipation of the initial crack.

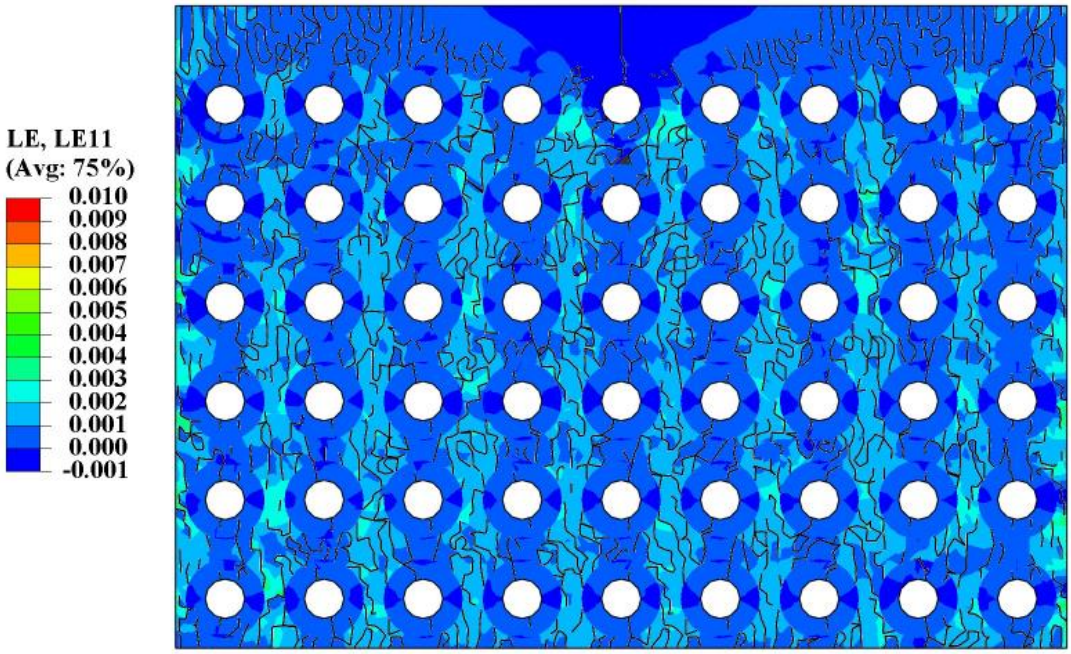

Fig. 16 The 1-directional strain distribution of the final stage of the fracture on dentin's microstructure, with elastic ITD.

In the last step of the crack propagation as shown in Fig. 16, the 1-directional strain is more evenly distributed on the ITD with a higher value on the 2-direction. Such specific high value on the 2-direction could be attributed to the special shape of PTD and the elastic modulus difference: under 1-directional tensile loading, with a circular shape when the surrounding soft matrix is under tension the PTD perpendicular axis (2-direction) is under compression, hence dissipate energy in the 2-direction to its surrounding soft matrix, ITD. Hence the ITD is compressed within the two PTDs, indicating 2-directional strain value concentration.

3.2.2 Plastic ITD

With the adoption of the perfectly plastic model of ITD, we generate different results with the beyond. Detecting these differences might unveil the mechanism of the ITD plastic nature.

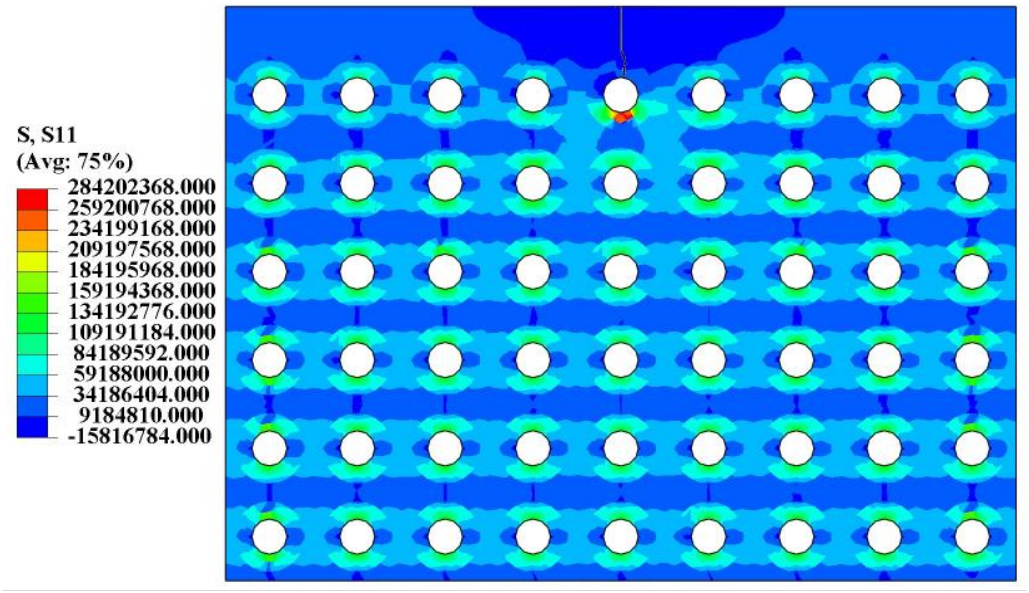

Fig. 17 The 1-directional stress distribution of preliminary stage of the crack propagation on dentin structure, with a perfectly plastic ITD, in first step.

In the preliminary stage, the stress distribution generally has no difference due to the plastic has not made much effect from Fig. 17. From Fig. 18 and Fig. 13 we detect similar crack propagation patterns, but fewer cracks in Fig. 18. Also, the structure displays a less 1-directional stress value shown in Fig. 18 with the plastic ITD. Such a phenomenon indicating the plasticity reduces the stress, and resist the crack growth comparing the 1-directional stress distribution.

Notably, a stress distribution difference occurs along the propagating of the initial crack comparing Fig. 18 with Fig. 13. The 1-directional stress distributed along the initial crack as a triangle area in Fig. 13, howbeit a stress decrease along the initial

crack as given in Fig. 18. Such distributions also indicate how the plastic ITD could reduce the stress and resist the crack growth.

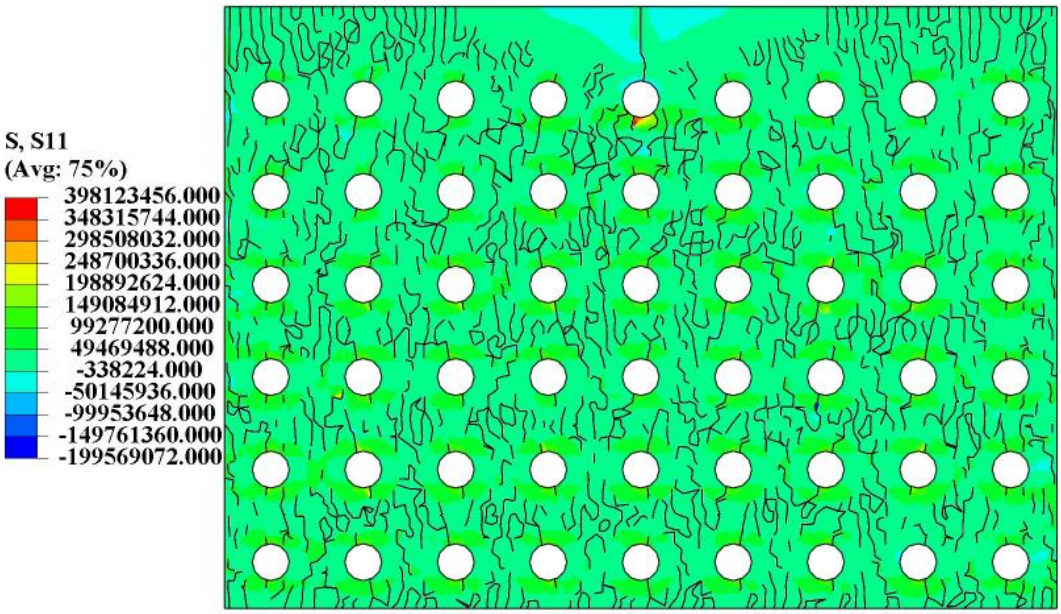

Fig. 18 The 1-directional stress distribution of the final stage of the fracture on dentin's microstructure, with a perfectly plastic ITD.

From Fig. 19 and Fig. 14 we observe conspicuous differences as the strain is comparably more concentrated along the 1-direction with the adoption of the plasticity. But the maximum strain value is lower for plastic ITD with 0.002 comparing with 0.003. Albeit the concentrated strain value along 1-direction is bigger than dentin with elastic ITD. The concentration in 1-direction at the beginning stage could be attributed to plasticity responding to tensile loading to resist fracture.

At the stage of the fracture initiation, a totally different 1-directional strain distribution displayed as given from Fig. 15 and Fig. 20. The elastic ITD model displays a higher maximum strain value. The general strain value variance between the ITD and PTD is similar for the two models. Howbeit the plastic ITD model displays higher 1-directional strain value.

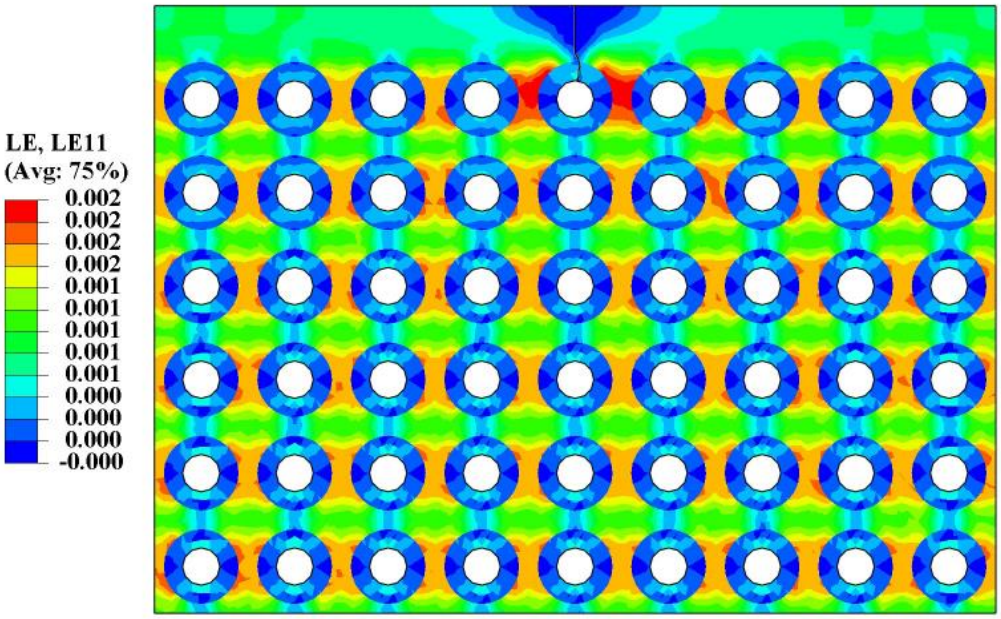

Fig. 19 The 1-directional strain distribution of preliminary stage of the crack propagation on dentin structure, with a perfectly plastic ITD.

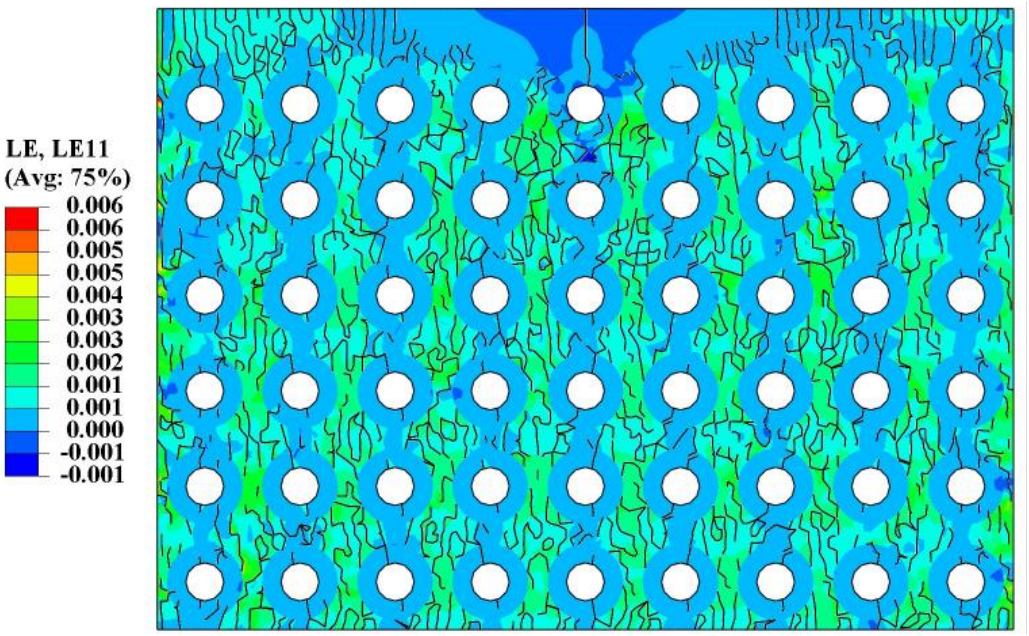

Fig. 20 The 1-directional strain distribution of the final stage of the fracture on dentin's microstructure, with a perfectly plastic ITD.

To specify the effect of the plastic nature from the ITD, we know present 1-directional plastic strain evolving from Fig. 21 to Fig. 22. The plastic strain does not exhibit a notable effect at the crack initiation stage in Fig. 21, with only small plastic strain, occurs on the ITD cracks bonding the PTD.

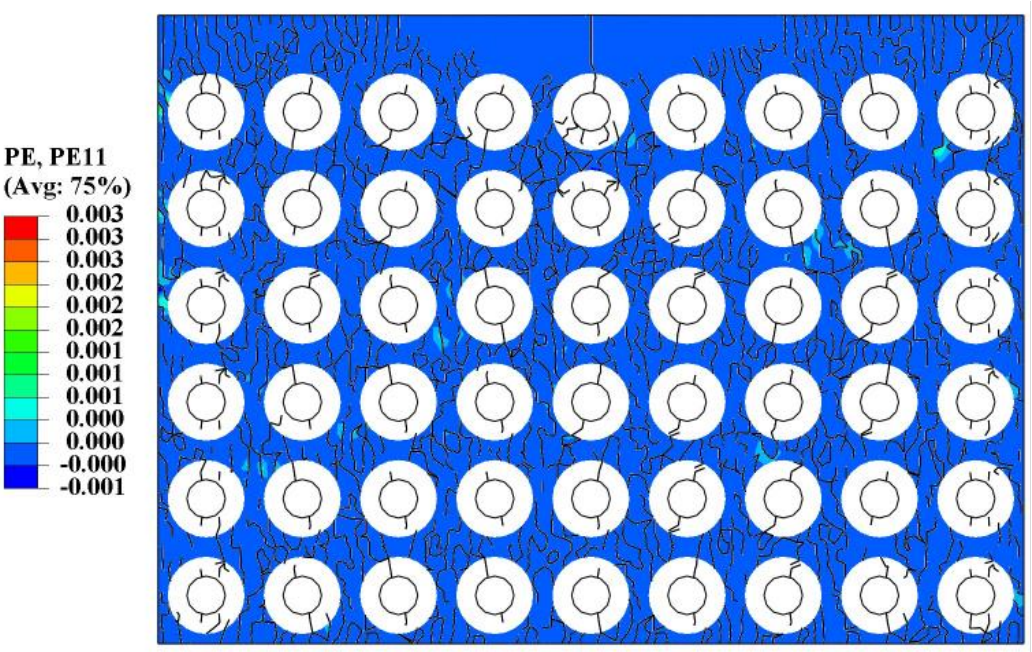

Fig. 21 The 1-directional plastic strain distribution, when the fracture initiate on dentin, with a perfectly plastic ITD.

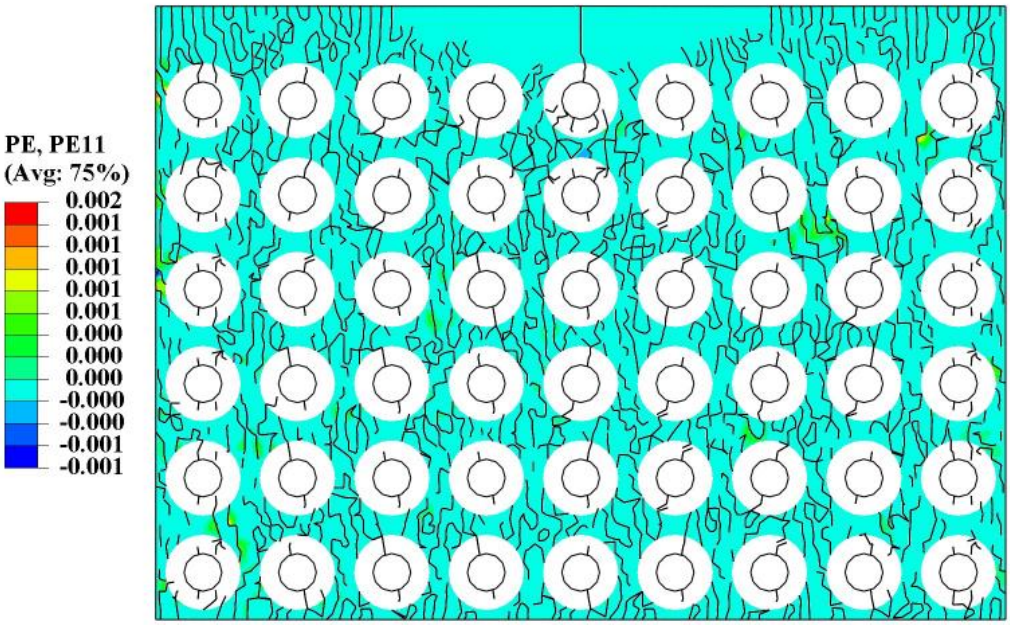

Fig. 22 The 1-directional plastic strain distribution of the final stage of the fracture on dentin's microstructure, with a perfectly plastic ITD.

As for the final stage of the crack propagation, the 1-directional plastic strain still does not display the conspicuous impact of the ITD. Yet the strains occur in several areas within the cracks for the value of approximately 0.001. As comparing and discussed previously, such plastic concentrate to resist crack and fracture. With

specifically show the 1-directional plastic strain distribution, one deduces the plastic strain does not make much variance on the total strain value, however, the plastic nature helps reduces stress increases and concentration, henceforth, releases fracture energy to resist crack growth.

To quantitatively show how plasticity alters the stress-strain distribution, here, we present 1-directional stress-strain diagrams for both the PTD and ITD considering elastic and plastic ITDs as given from Fig. 23 to Fig. 24. During the fracture process, for the elastic PTD, with an elastic ITD, the PTD displays higher 1-directional values shown in Fig. 23, indicating the plastic ITD could reduce the 1-directional stress on the bonding PTD. Such results indicate the plastic nature of ITD can release stress and reduces chances for fracture on the PTD. In the zoomed view shown in Fig. 23, the 1-directional stress initially growing with the same trends growing with the slops with an approximately higher stress value, then exhibits a higher slope with a higher stress.

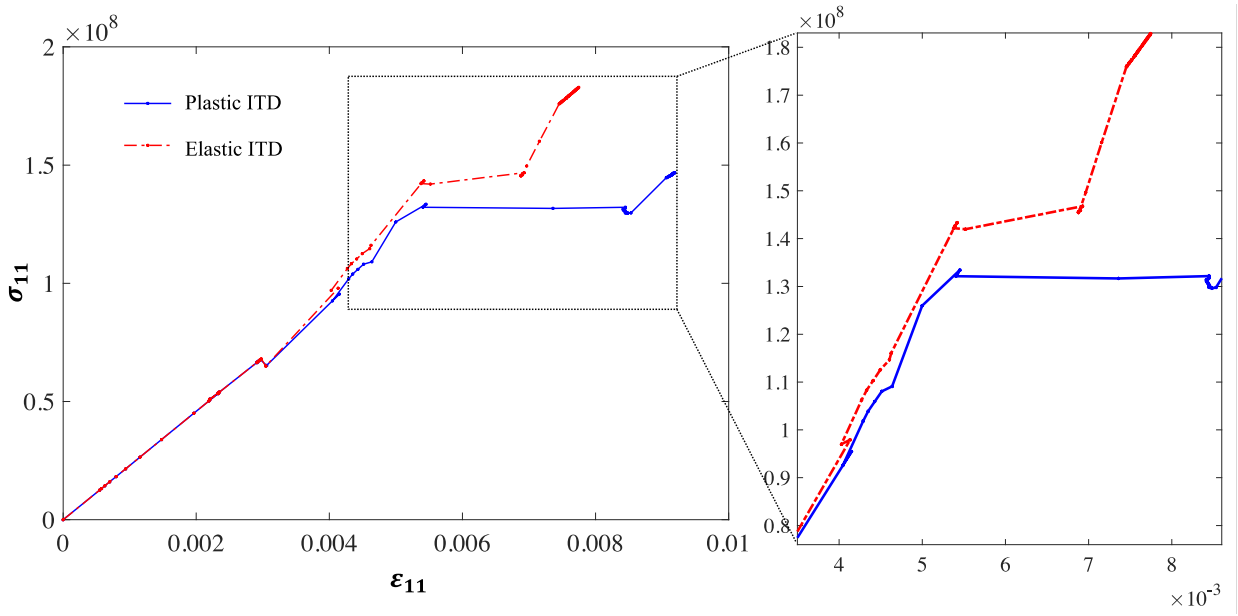

Fig. 23 The 1-direction stress-strain relationship of the PTD with the crack propagation, comparing elastic and perfectly plastic ITD, respectively.

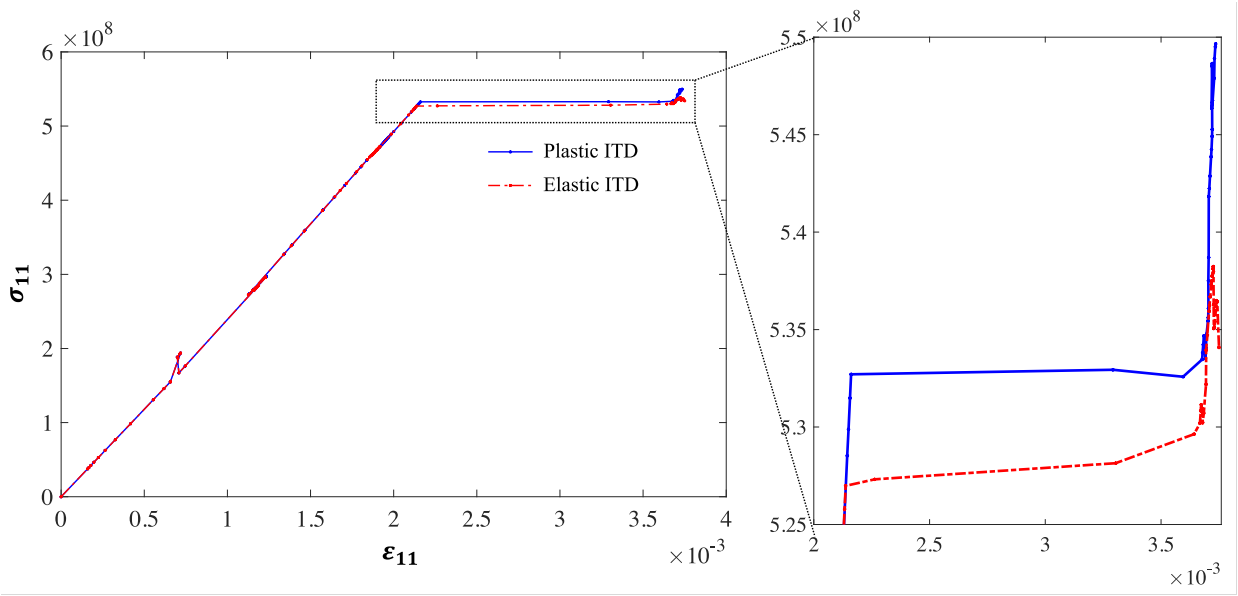

Fig. 24 The 1-direction stress-strain relationship of the ITD with the crack propagation, comparing elastic and perfectly plastic ITD, respectively.

Here in Fig. 24, the plastic nature does not variate the 1-directional stress as shown clear for PTD in Fig. 23. Only little variance can be detected after the initiation of the fracture as small 1-directional stress difference shown in the zoomed view in Fig. 24.

Comparing Fig. 23 and Fig. 24 we deduce that the plasticity of ITD will robustly affect the 1-directional stress distribution of its bonding PTDs, howbeit will not alter such distribution for ITD. Hence, we can reason out the protection mechanism of the ITD plasticity: to reduce the tensile stress on the PTD to avoid PTD crack as mentioned in the preceding chapter, thence the crack is less likely to propagate along the PTD to ITD to cause further fracture and failure.

As mentioned in the §1, the debonding of the ITD and PTD is caused by the elastic modulus mismatch of the two materials, which occurs along the bonding interface. In our approaches, no clear debonding phenomena observed howbeit similar fracture

observed as in the zoomed view in Fig. 12 and Fig. 15. Hence, the debonding can be investigated based on our model through studying the shear stresses on the bonding interface between the ITD and PTD.

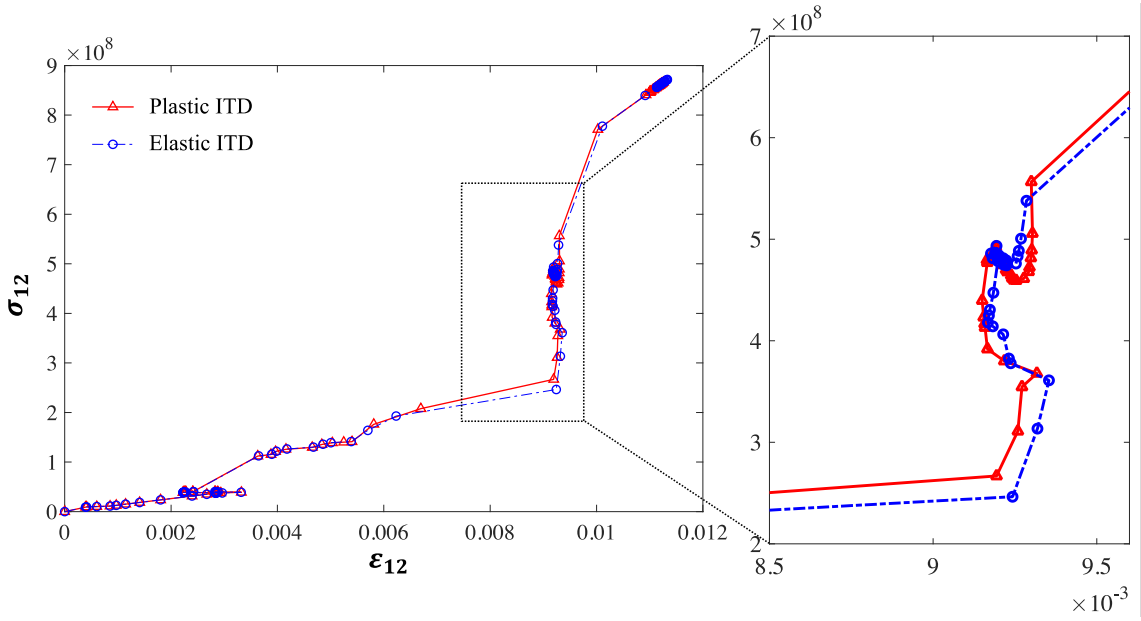

Fig. 25 The shearing stress-strain relationship of the bonding interface with the crack propagation, comparing elastic and perfectly plastic ITD, respectively.

Here, in Fig. 25, the shear stress-strain on the ITD and PTD bonding interface is given. From the distribution of the diagram, there is no clear variance with the effect of the ITD plasticity. With the scrutiny of the two curves, the zoomed view displays small variance with the two stresses, in which the plastic ITD bonding shearing stress was initially larger but later smaller than the elastic ITD's, and later on bigger than the elastic ITD. The competing stresses as shown on the bonding interface within the plastic and elastic ITD clue in that plasticity does not alter shearing between boundaries or frictional failure for our model. Also, the competing stresses indicate how elastic and plastic ITD show different bonding friction behavior at different phase with a generally similar trend.

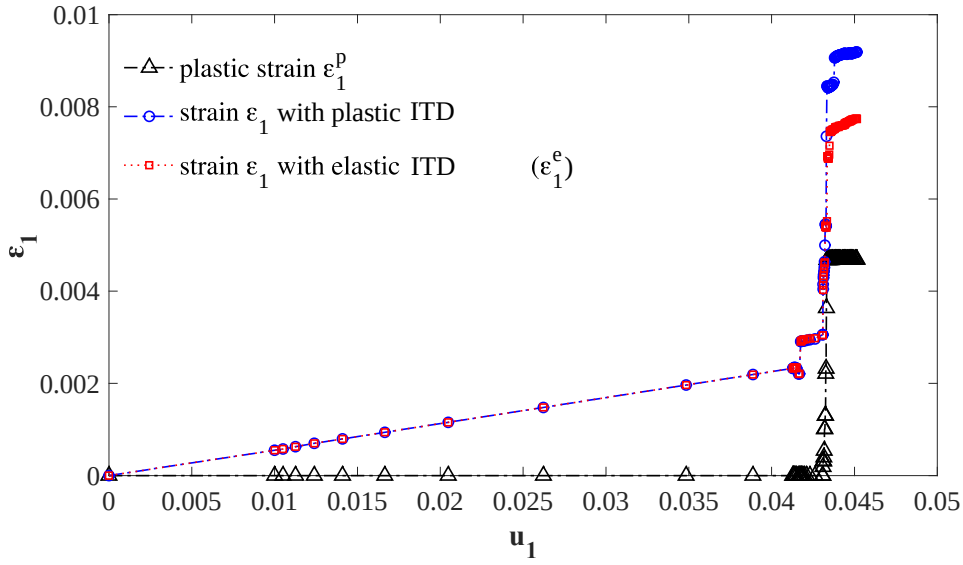

Fig. 26 The 1-directional strain evolution with the growing 1-directional displacements, in which the plastic strain, total strain of the elastic and perfectly elastic ITD is presented respectively.

As shown in Fig. 14 to Fig. 16 and Fig. 19 to Fig. 22, aside from previous discussions, Fig. 26 quantitatively presents how plasticity affects the 1-directional strain distribution in the fracture process. The curves comparing structure with the 1-directional strain of the plastic ITD, elastic ITD, and the plastic strain presents how strain evolves in the fracture process. Both the 1-direction strain for elastic and plastic ITD experience a ladder-shaped increase as the 1-directional displacement in the value of about 0.042. Subsequently, the plastic strain makes an effect at the displacement value of about 0.043. The ladder-shaped strain increase indicates the fracture occurs on dentin. With the effect of the ITD plastic strain, the dentin structure experience overall higher strain value as to resist crack. Observing the details, there is a smaller ladder-shaped increase for the dentin strain with plastic ITD. Such ladder-shaped increasing of the strain could also attribute to the protection mechanism of the plasticity as to resist crack growth.

4 Conclusion

Investigating the stiffness and toughness of the dentin structure, we first model the geometry based on the dentin microstructure from SEM photos (Fig. 1, Fig. 2). The study of the composite's elastic modulus based on Eq. 2 to Eq. 4 with the boundary conditions of tensile loading with fixed displacement in 1-direction as shown in Fig. 3 and depicted in Eq. 1. Considering the elasticity and plasticity (Eq. 5 to Eq. 7) of ITD respectively regarding parameters of Tab. 2. The fracture of the structure is based on adopted ductile damage evolution model with failure criterion of maximum principal stress (Eq. 9 to Eq. 14) with specific parameters (Tab. 3 to Tab. 6) and boundary conditions of fixed on the down edge under tensile loading with an initial crack (Fig. 4 and Eq. 15).

We obtain results of the dentin composite's elastic modulus 1765574656 Pa. The 2-directional stress distribution shows there are stress concentrations along the axis perpendicular to the loading directions on PTD (Fig. 6). The 2-directional strain also exhibits similar behavior (Fig. 5). With ITD plasticity, the 2-directional strain is more heavily concentrated on the four corners bonding the PTD on ITD (Fig. 7). Such phenomenon is delineated through observing the 2-directional plastic strain distribution, showing the plastic strain initiated on the four corners nearing the central axis, from which we could deduce the strain concentrations on corners are ITD plastic effect (Fig. 8). The 2-directional stresses exhibit lower values with more an evenly distributed pattern (Fig. 9). The 2-directional reaction forces visualize how ITD plasticity influences the overall stiffness through forces reduction (Fig. 10).

For the fracture growth evolution, we observe two types of cracks: crack growing along the axis perpendicular to the loading direction on PTD and wavy cracks surrounding the PTD on ITD as in the zoomed views (Fig. 12 and Fig. 15). We also detected V-shaped cracks (Fig. 15) that can be attributed to the synergy of the PTD inner friction and crack propagation along the axis perpendicular to the loading direction. With the plasticity of ITD, the structure exhibits lower 1-directional stress values (Fig. 13 and Fig. 18) yet small variance for the 1-directional strain (Fig. 16 and Fig. 20). To investigate the plasticity specifically, the 1-directional plastic strain shows little concentration on ITD with a value of approximately 0.001 (Fig. 21 to Fig. 22). Such a result indicates the plastic strain does not variate strain value evidently, while reduces the stress value to resist crack growth (Fig. 18 and Fig. 13).

Based on the 1-directional stress-strain distribution for both the ITD and the PTD, The ITD plasticity reducing the PTD with elastic ITD for 2-directional stress evidently in Fig. 23. Howbeit the ITD plasticity slightly increases the ITD 2-directional stress value (Fig. 24 and Fig. 25). Such results unveiled the protection mechanism of ITD plasticity: to slightly increase the ITD stress to absorb the fracture energy dissipated from the PTD as the PTD stress is reduced. There is no shearing stress value variance on the bonding interface, indicating plasticity does not contribute to such fracture phenomenon (Fig. 25). The strain distributions indicate plasticity occurs after the initiation of fracture to resist further failure (Fig. 26).

Acknowledgement

The author would like to thank B. An for the valuable discussion.

References

[1] D. Arola, S. Gao, H. Zhang, R. Masri. The Tooth: Its Structure and Properties. Dental Clinics of North America. Volume 61, Issue 4, October 2017, Pages 651-668.

[2] Marshall GW Jr. Dentin: microstructure and characterization. Quintessence Int. 1993; 24(9):606-617.

[3] Jacob Lubliner [1990]. PLASTICITY THEORY.

[4] Z. Suo. Perfect Plasticity. Plasticity. imechanica.org.

[5] Jinyuan Zhai. MODELING DUCTILE DAMAGE OF METALLIC MATERIALS. PhD Dissertation. University of Akron. August, 2016.

[6] J. Ruzicka, M. Spaniel, A. Prantl, J. Dzugan, J. Kuzelka, M. Moravec. Identification of Ductile Damage Parameters in the Abaqus. March 2013.

[7] D. Arola, J. A. Rouland, D. Zhang. Fatigue and fracture of bovine dentin. Experimental Mechanics volume 42, pages380–388(2002)

[8] J. Ivanci, M. Naranjo, S. Correa, A. Ossa, F.R. Tay, D.H. Pashley, D. Arola. Differences in the microstructure and fatigue properties of dentine between residents of North and South America. archives of oral biology 59 (2014) 1001–1012

[9] Zhang, Y., Du, W., Zhou, X. et al. Review of research on the mechanical properties of the human tooth. Int J Oral Sci 6, 61–69 (2014).

[10] M. Toparli, N.S. Koksal, Hardness and yield strength of dentin from simulated nano-indentation tests, Computer Methods and Programs in Biomedicine, Volume 77, Issue 3, 2005, Pages 253-257, ISSN 0169-2607

[11] Amaury Namour et al. Treatment of Dentinal Hypersensitivity by means of Nd:YAP Laser: A Preliminary In Vitro Study. The Scientific World Journal. Volume 2014, Article ID 323604, 7 pages

[12] A. Nazari, D. Bajaj, D. Zhang, E. Romberg, D. Arola. Aging and the reduction in fracture toughness of human dentin. JOURNAL OF THE MECHANICAL BEHAVIOR OF BIOMEDICAL MATERIALS 2 (2009) 550–559.

[13] B. An, H. D. Wagner. Role of microstructure on fracture of dentin. Journal of the Mechanical Behavior of Biomedical Materials. Vol 59 (2016): 527-537. ISSN 1751-6161.

[14] An B. Constitutive modeling the plastic deformation of bone-like materials. Int J of Solids Struct 2016; Vol 92–93: 1-8

[15] An B., Zhang D. Bioinspired toughening mechanism: lesson from dentin. Bioinspir. Biomim., 10 (2015), Article 046010

[16] B. An, D. Zhang. An analysis of crack growth in dentin at the microstructural scale. Journal of the Mechanical Behavior of Biomedical Materials 81 (2018) 149–160.

[17] B. An, Y. Xu, D. Zhang. Crack initiation and propagation in composite microstructure of dentin. International Journal of Solids and Structures 110–111 (2017) 36–43

[18] H. Teng. Effective elastic–plastic response of two-phase composite materials of aligned spheroids under uniaxial loading. Mechanics of Materials 117 (2018) 91–104.

[19] M. Majewski, P. Holobut, M. Kursa, K. Kowalczyk-Gajewska. Packing and size effects in elastic-plastic particulate composites: Micromechanical modelling and numerical verification. International Journal of Engineering Science 151 (2020) 103271

[20] C. He, J. Ge, B. Zhang, J. Gao, S. Zhong, W. K. Liu, D. Fang. A hierarchical multiscale model for the elastic-plastic damage behavior of 3D braided composites at high temperature. Composites Science and Technology 196 (2020) 108230

Highlights

- The fracture mechanism of the dentin structure is elucidated.
- The failure evolution of the dentin structure is presented.
- The influence of the ITD's plastic nature on the dentin's mechanical distribution is given.
- The protection mechanism of the ITD's plastic nature is unveiled.